RSC Advances

ROYAL SOCIETY OF CHEMISTRY

www.rsc.org/advances

Strong, Flexible and Thermal-Resistant CNT/Polyarylacetylene Nanocomposite Films

Wenfu Cai,[a] Min Li,*[a] Shaokai Wang,[a] Yizhuo Gu,[a] Qingwen Li[b] and Zuoguang Zhang[a]

a. Key Laboratory of Aerospace Advanced Materials and Performance (Ministry of Education), School of Materials Science and Engineering, Beihang University, No. 37 Xueyuan Road, Haidian District, Beijing 100191, China. E-mail: leemy@buaa.edu.cn; Fax: +86-10-82339800

b. Suzhou Institute of Nano-Tech and Nano-Bionics, No. 398 Ruoshui Road, Suzhou 215123, China.

Abstract

This paper reports a new nanocomposite in combination of high char yield polyarylacetylene (PAA) resin and ductile carbon nanotube (CNT) film. Benefited from the big specific surface area and excellent mechanical properties of CNT film, the resultant nanocomposite conquers the shrinkage and crack defect of neat PAA. This nanocomposite has great flexibility and tensile strength and modulus of 303±38 MPa and 22±2 GPa respectively. The through-thickness thermal conductivity of CNT film/PAA composite reaches 1.15W/(mK), seven times higher than pristine CNT film, and the electric conductivity increases to 700 S/cm. Meanwhile, a lock-up effect of PAA on CNT network ensures good stability of the structure. TG test demonstrates that in comparison with CNT film/epoxy composite, CNT film/PAA has significantly high decomposition temperature with the char yield up to 90.7%. After a carbonization at 900°C for 0.5h, the nanocomposite remains the tensile strength over 66%.

Keywords: carbon nanotube film; polyarylacetylene; heat-resistant resin; thermal conductivity

Introduction

Carbon nanotube (CNT) film has been well-known for its extraordinary mechanical and physical performance. CNT film, which is made of inter-tangled CNTs, is one of the most promising macroscopic form. It inherits the advantages of individual carbon nanotubes, such as high strength and modulus, remarkable electrical and thermal conductivity[1-3] with low density and high specific surface area. As a multi-functional reinforcement, the CNT film has been impregnated with epoxy or bismaleimide (BMI) resin to prepare structural and functional materials. Li *et al*[4] fabricated a CNT film/epoxy composite by resin solution impregnation, which showed high tensile strength and toughness of 405 MPa and 122 J/g, as well as excellent damping properties. Wang *et al*[5] prepared aligned CNT film/BMI composite with high CNT fraction to achieve a tensile strength of 3.8 GPa, and Young's modulus of 293 GPa. These composites have low glass transition temperature due to the polymer matrixes. Some attempts have been made to improve the heat-resistant property by combining phenolic resin. An *et al*[6] found that thermal decomposition temperature was enhanced greatly through dispersing 1.5 wt% CNTs into phenolic resin with a char yield of 62.5% left. Moreover, Tai *et al*[7, 8] reported that CNT network produced good mechanical properties for its phenolic composites with a tensile strength of 80 MPa and a Young's modulus of 7.5 GPa. However, the char yield of common phenolic resin (<60%) still cannot meet the requirement for higher thermal stability[9, 10].

As a highly cross-linked aromatic polymer containing only carbon and hydrogen, polyarylacetylene (PAA) has excellent heat-resistant property, and better ablation stability than phenolic resin[11, 12]. The char yield of PAA can reach 80-85%, and PAA has lower shrinkage during pyrolysis and moisture absorption[13, 14]. Thus PAA is an ideal resin for high temperature applications. However, during PAA polymerization, large curing exotherm and rapid reaction rate may cause flash polymerization even explosion[15]. Moreover, PAA is brittle and has low structural integrity due to its highly cross-linked structure[16]. Besides, non-polar feature of PAA often causes weak interfacial adhesion with reinforcement[17]. It remains a challenge to prepare defect-free PAA composite to fully utilize its heat-resistant properties. By combining CNT film and PAA resin and taking advantage of the former's high specific area, superb

toughness and excellent mechanical and functional properties, it is promising to overcome the shortcomings of PAA and improve thermal performance of the nanocomposite at the same time.

In this paper, a CNT film/PAA composite is successfully prepared to explore a new way to merge strong points for CNT network and PAA resin. The effects of CNTs on the curing characteristics and shrinkage of PAA are analysed, and mechanical properties and thermal and electrical conductivity of the nanocomposite are investigated. Moreover, the degradation of CNT film/PAA composite under high temperature and its influence on the nanocomposite's properties are highlighted to reveal its heat-resistant performance.

Experimental

Materials

CNT film was synthesized through floating catalyst chemical vapor deposition (FCCVD) method. The detailed manufacturing process of CNT film has been reported in our previous research[4, 18, 19]. These fabricated CNTs have a diameter of 6-10 nm with 3-8 walls. The pristine CNT film are randomly oriented with an average thickness of 30 μm. It can be aligned via a simply mechanical stretching process by using a tensile machine (Instron 5565) with a load cell of 5kN. To achieve a higher stretching ratio, 75 wt% ethanol and water solution was uniformly sprayed on the CNT film during stretching. The stretching speed was controlled at 2 mm/min. In this research, the aligned CNT film with a draw ratio of 35% was prepared for the fabrication of polymer nanocomposites.

PAA resin was produced by East China University of Science and Technology. The resin has a density of 1.03 g/cm^3 at ambient temperature. The chemical purity acetone was produced by Beijing Chemical Works. Epoxy resin E51 was produced by Bluestar New Chemical Materials Co. Ltd. The E51 epoxy resin is bisphenol-A diglycidyl ether type (DGEBA) with epoxy value of 0.48-0.54. The hardener of 2-ethyl-4-methyl imidazole was produced by Beijing Xiangshan United Assistant Factory. The mixing mass ratio of resin to hardener was 100:7.

Preparation of CNT film/PAA composite

CNT film/PAA composite was prepared by solvent dipping process. Firstly, CNT film was cut into rectangles with the dimension of 40×60 cm^2 and then soaked into PAA/acetone solution for 1 hour. The CNT film composites impregnated with 5 wt% and 15 wt% PAA solution were denoted as CNFP5 and CNFP15. The fully impregnated CNT film/PAA prepreg was placed in vacuum oven at 40 °C for 0.5 hour to remove acetone. To prepare composite, the CNT film prepreg was sandwiched into two pieces of polytetrafluoroethylene film, and then they were placed in steel mold. Hot-press method was applied to compact the CNT stack and cure the resin. The temperature schedule was 115°C/10h +120°C/4h +140°C/2h +160°C/2h +180°C/2h +250°C/4h and curing pressure was controlled at 10MPa. After CNT film/PAA composite was cured, the whole assembly was naturally cooled to room temperature.

In comparison, CNT film composite impregnated with 5wt% epoxy solution was also prepared by solvent dipping process above. The temperature schedule was 80°C/1h +125°C/2h and curing pressure was controlled at 10MPa.

Based on thermogravimetric test, the pristine CNT film remained 21.9 wt% after experiencing 900°C in air. Thus the content of Fe catalyst in CNT film is calculated to be 15.3 wt%. According to the mass loss of CNT film before 350°C, there are about 2.6 wt% oligomers in the CNT film. Hence the content of CNTs in pristine CNT film is about 82 wt% and the CNTs content in the nanocomposites can be inferred in accordance (Table. 1).

Table. 1 Resin and CNTs content of different CNT film nanocomposites.

Name	Sample	Resin content (%)	CNTs content (%)
CNF	CNT film	0	82
CNFP5	Nanocomposite from 5 wt% PAA solution	35±5	53±5
CNFP15	Nanocomposite from 15 wt% PAA solution	65±7	29±7
CNFE5	Nanocomposite from 5 wt% epoxy solution	43±6	47±6

Characterization

The curing characteristics of PAA and the nanocomposites were characterized by a differential scanning calorimeter (Mettler DSC-1) at a heating rate of 10°C/min. Their decomposition temperature and char yields were measured by thermogravimetric analyser (Mettler TGA-1) in air and N_2 atmospheres at 10°C/min, respectively.

The surface morphologies of CNT film and the nanocomposites were observed by a JEOL JSM-7500F scanning electron microscope (SEM).

For the measurement of tensile properties, the nanocomposites were cut into 25×2 mm^2 rectangular strips. Instron 5565 with a 500 N load cell was used. The clamping distance was 20 mm and the sample thickness was measured by a micrometer caliper. The displacement was controlled at 0.5 mm/min.

The degree of orientation of CNTs in aligned CNT film can be measured using polarized Raman spectroscopy (Renishaw RM2000). The intensities of the G-band were recorded when the incident laser beam (514 nm) was respectively placed parallel and perpendicular to the alignment direction of the CNT film. The ratio of $I_{G\parallel}/I_{G\perp}$ was adopted to describe the orientation degree of CNTs.

Electrical conductivity was measured by four-probe conductivity meter (RTS-9, 4probes tech, Inc.). Thermal conductivity was tested by a laser flash thermal analyzer (LFA447, NETZSCH, Inc.). The monolayer nanocomposite film was attached to a 0.3 mm thick aluminum sheet to meet the thickness requirement. A double-layer mode in the testing software was selected to measure the through-thickness thermal diffusivity. Thermal conductivity can be calculated by the following equation:

$$\lambda=\alpha\times Cp\times\rho \quad (1)$$

Wherein α is the thermal diffusivity, Cp is specific heat capacity and ρ is the density. In-plane and through-thickness thermal diffusivities of eight-layered CNT film/PAA composite can be measured directly by selecting the single layer mode of the testing software.

Results and discussion

Effect of CNT network on curing shrinkage of PAA

Fig. 1 compares the morphology of neat PAA casting, carbon fiber/PAA composite, and CNT film/PAA composite. PAA casting is extremely difficult to prepare because its shrinkage ratio can reach 11.7%. The neat PAA often cracks into pieces after curing as shown in Fig. 1a. Even in carbon fiber reinforced PAA composite, micro-cracks can be often observed[20], as shown in Fig. 1b. These crack defects are closely related to the large curing exotherm and highly cross-linked structure of PAA matrix. PAA is mainly composed of p-diethynylbenzene, m-diethynylbenzene and solvents. After curing, highly cross-linked structures of cis conjugated polyene and polyphenylene are formed, as shown in Fig. 2. Both solvent vaporization and high cross-linking density cause the shrinkage of PAA.

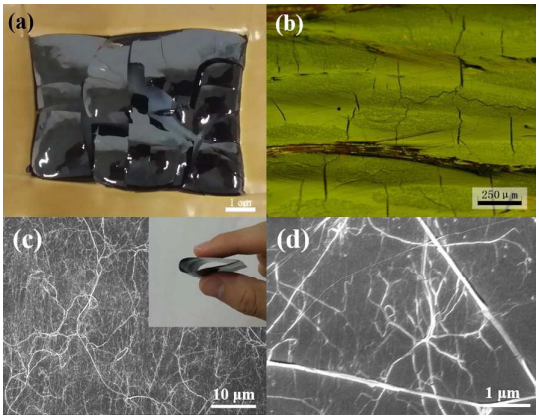

Fig. 1 Morphology of (a) cracked PAA casting, (b) micro-cracks in carbon fiber/PAA composite and (c) CNFP5 inserted with bended nanocomposite film and (d) its enlarged image.

On the contrary, the CNT film reinforced PAA composite shows neat surface (as shown in Fig. 1c and 1d), which indicates that compatible combination of PAA and the CNT network forms a nanocomposite without macro or micron-size defects. Hence, we can infer that the CNT network can effectively restrict the shrinkage of PAA matrix. Moreover, benefited from the super ductility of carbon nanotubes, this CNT/PAA film is very flexible. This film can be easily bent, and no crack is observed after the shape recovery.

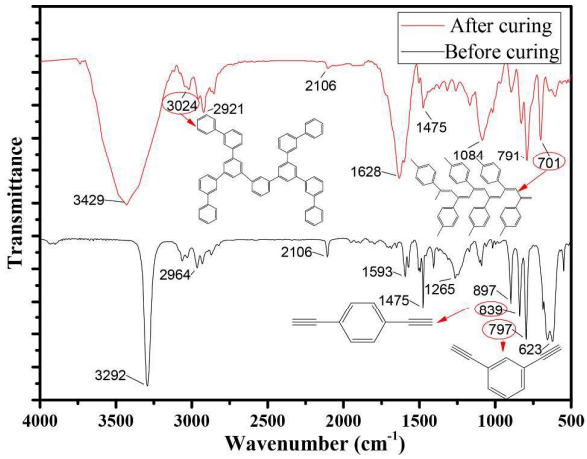

Fig. 2 Infrared spectrums of PAA before and after resin curing.

In order to reveal the effect of CNT on the crack elimination in PAA matrix, the morphology of CNT film and the curing characteristics of CNT film/PAA composite were investigated. The pristine CNT film is porous with an average pore diameter of approximately 45 nm (as illustrated in Fig. 3a), which effectively separates PAA matrix into nanoscale domains. The contact angle between 15 wt% PAA solution and CNT film is only 6.4°, showing excellent wettability for PAA resin with CNT film, even better than epoxy resin[4]. This suggests that PAA resin can easily infiltrate the nanoscale pores to avoid resin enrichment on the surface. Fig.3b further illustrates the curing characteristics of neat PAA and PAA matrix in CNT film. Neat PAA has a sharp exothermic peak with a heat release of 513J/g. The PAA matrix in CNT film shows a gentle DSC profile suggesting distinct stereo-hindrance effect of CNT network to retard PAA's polymerization. This phenomenon was also reported in CNT/epoxy composites[21]. Lower crosslink density of PAA in the CNT film tends to result in lower shrinkage ratio. Besides, high thermal conductivity of CNT network also helps to transfer the reaction heat to avoid heat accumulation. All these factors contribute to the CNT film/PAA composite without macro or micron-size defects.

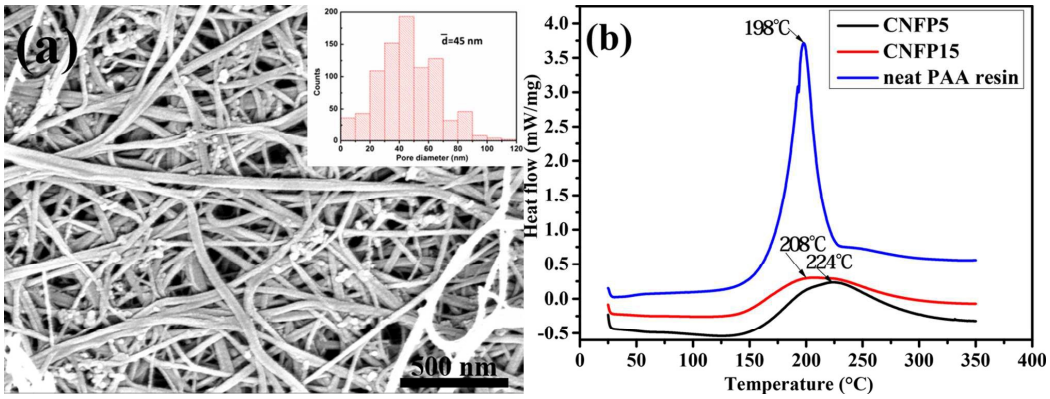

Fig. 3 (a) Porous structure of CNT film inserted with pore diameter distribution; (b) Curing exothermic curves of neat PAA and different CNT film/PAA composite.

Tensile properties of CNT film/PAA and its high temperature performance

Fig. 4 shows the tensile stress-strain curves of CNT film/PAA composites, CNT film/epoxy composites and pristine CNT film. The stress-strain curves of CNT/PAA and CNT/epoxy are quite different. PAA nanocomposite exhibits much higher modulus but smaller strain at breakage than CNT/epoxy. CNFP5 shows two stages: an initial linear stage (I) and a following stage with slight inflection (II). In comparison, the CNT film impregnated with 5wt% epoxy (CNFE5) went through three main stages before break: The first linear stage with the tensile strain less than 1%; the second stage with the occurrence of inflection (1%<ε<5%); and the third stage with a slow stress increase until break[4]. Moreover, pristine CNT film shows similar tendency as CNFE5. Higher modulus and wider linear strain of PAA nanocomposite mean better network stability than CNT/epoxy. This is also the reason for shape recovery of PAA composite without plastic deformation of CNT network.

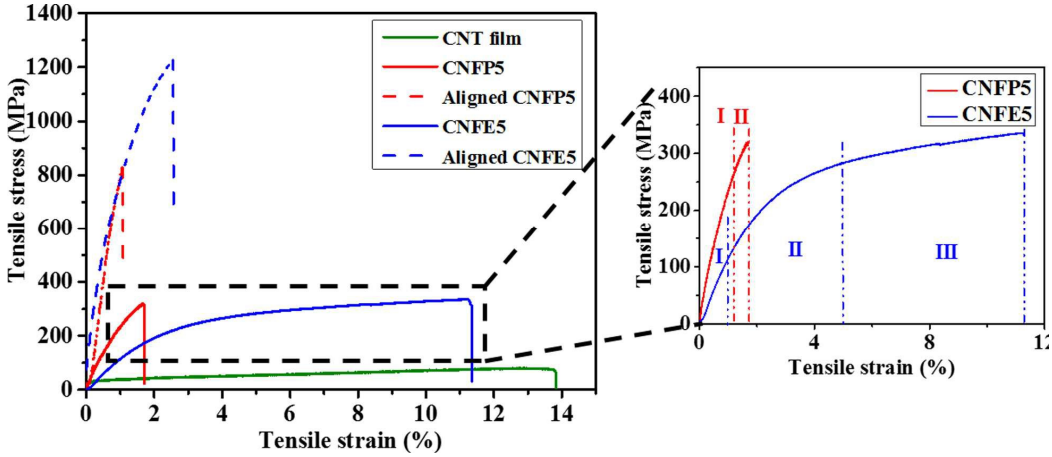

Fig.4 Tensile stress-strain curves of pristine CNT film, PAA and epoxy nanocomposites

As regards the mechanical properties, CNFP5 shows a tensile strength of 303±38 MPa, Young's modulus of 22±2 GPa, and toughness of 5.5 J/g. Comparatively, CNFE5 has a tensile strength and modulus of 281±36 MPa and 11±4 GPa, and toughness of 49 J/g. When CNT film is soaked in PAA solution with a higher concentration of 15 wt%, the tensile strength and modulus of CNFP15 decrease slightly to 157±26 MPa and 21±4 GPa as shown in Fig. 5. In order to improve the orientation of the CNTs, mechanical stretching is applied on the CNT film, and the degree of orientation $I_{G//}/I_{G\perp}$ is 9.1. Aligned CNT/PAA composite shows a completely linear relationship between tensile stress and strain as in Fig. 4. Correspondingly, tensile strength and modulus of the aligned CNFP5 increased by 270% and 460% to 830±58 MPa and 101±6 GPa respectively. Likewise, the aligned CNFP15 has higher tensile strength and modulus than the random CNT film composite, increasing by 430% and 395% respectively.

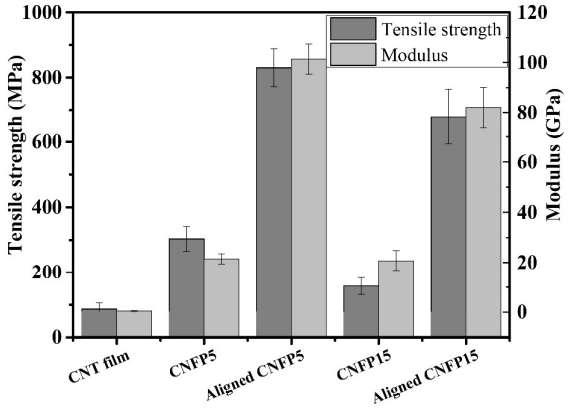

Fig. 5 Tensile strength and modulus of CNT film/PAA composites.

Fracture morphologies of different nanocomposites were also observed (Fig. 6). The CNT film/PAA composite shows random and crooked pull-out CNTs in the fracture with an average length only about 14 μm (Fig. 6b). For CNT film/epoxy composite, the pull-out CNTs become highly aligned with a longer length about 20 μm (Fig. 6a), which presents a typical ductile failure mode. The fracture toughness (K_{IC}) of PAA and epoxy casting measured by indentation microfracture method[22] are 1.85 MPa·$m^{1/2}$ and 4.58 MPa·$m^{1/2}$, respectively. This indicates that epoxy resin has a better ductility while PAA is brittle. Fig. 7 illustrates a strain-induced deformation during tensile test for PAA and epoxy composites. When the tensile force is loaded, the ductile epoxy nanocomposite greatly deforms and the slippage of CNTs occurs. The strain-induced alignment causes the significant yield before break. In comparison, the brittleness of PAA restrains the deformation of CNT network, and alignment can be hardly induced. As a result, a brittle failure mode predominantly happens. Hence, CNT film/PAA composite inherits the flexibility of CNT film and good rigidity of PAA matrix to achieve a flexible and strong composite film.

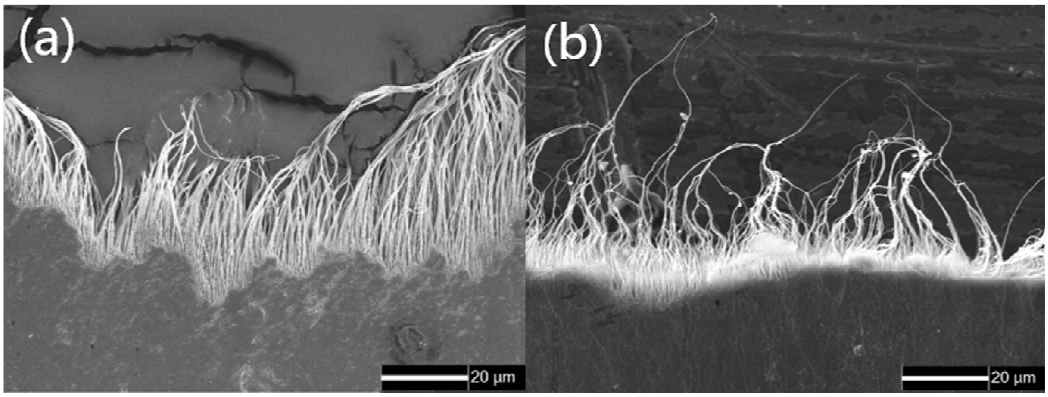

Fig. 6 Fracture morphologies of (a) CNT film/epoxy and (b) CNT film/PAA composite

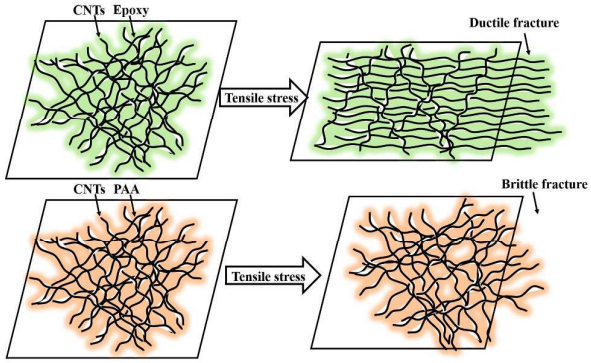

Fig. 7 Schematic diagram of ductile fracture mode of epoxy nanocomposite and brittle fracture mode of PAA nanocomposite.

It is known that PAA has a high char yield over 80%. High temperature treatment can further densify the PAA matrix. Thermogravimetric (TG) characteristics of the nanocomposites were analysed as shown in Fig. 8. The pristine CNT film decomposes slightly at 239°C in N_2 atmosphere due to the pyrolysis of oligomers produced by catalyst side reaction in the synthesizing process (Fig. 8a). After the introduction of PAA, the decomposition temperature at 5% mass loss of CNFP5 is 514°C with a char yield of 90.7% (see Fig. 8b). Comparatively, the decomposition temperature of CNT film/epoxy composite (CNFE5) is 383°C with a char yield only 58.1%. It is because neat PAA has good heat-resistance with a decomposition temperature over 500°C. The all carbon structure of CNT leads to a char yield over 94.5% of pristine CNT film, and thus the char yield of CNFP5 is higher than neat PAA. The high char yield ensures the minimal shrinkage of PAA nanocomposite during pyrolysis. As a result, both the effects of PAA and CNT film contribute to the excellent heat-resistant performance of PAA nanocomposite.

In air atmosphere (Fig. 8c), the temperature at maximum degradation rate of CNFP5 and CNFP15 are 605°C and 546°C respectively, higher than epoxy/CNT and BMI/CNT composite[23]. The multi-walled CNTs in the network have multiple layers to be burned through, and thus the pristine CNT film is less exposed to oxidative damage with a degradation temperature over 600°C. Hence the CNT network provides the composite with a good thermo-oxidation stability.

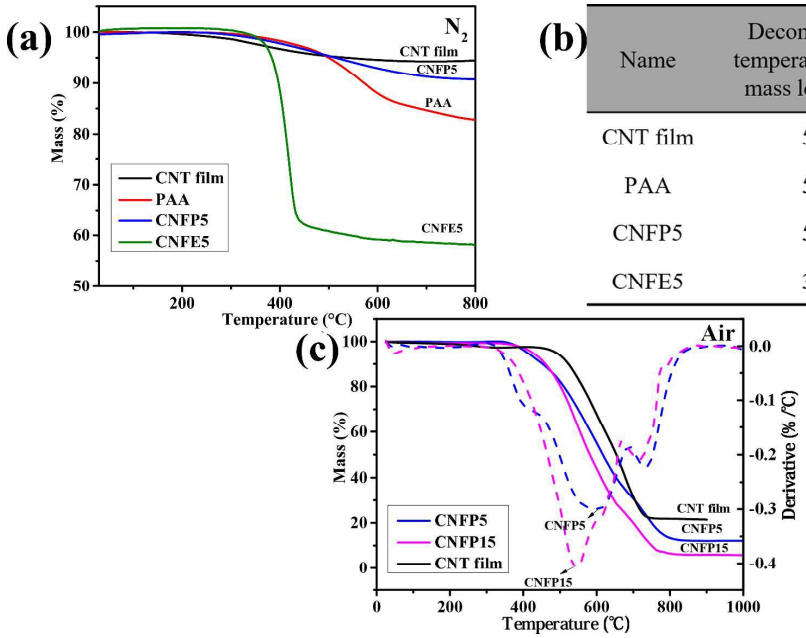

Name	Decomposition temperature at 5% mass loss (°C)	Char yield (%)
CNT film	538	94.5
PAA	507	82.7
CNFP5	514	90.7
CNFE5	383	58.1

Fig. 8 (a) TG curves and (b) the decomposition temperature and char yield of CNT film, PAA resin, and the CNT film nanocomposites in N_2 atmosphere; (c) TG and DTG curves of CNT film/PAA composites in air.

In order to further reveal the potential of PAA nanocomposite for ablative material, its retention rate of tensile property was measured after carbonization treatment. Thus a heat treatment at 900°C in N_2 for 0.5h was adopted to make PAA fully carbonized[24]. In Fig. 9a, the carbonized CNFP5 shows a tensile strength of 210 MPa with a retention rate of 66%. The Young's modulus of the carbonized CNFP5 decreases slightly to 19.7 GPa from 22.3 GPa. The stress-stain curves in Fig. 9a show no obvious yield before failure and the elongations decrease significantly after carbonization. In Fig. 9b, the fracture of the carbonized nanocomposite is neat and smooth with minimal long pulling-out CNTs, which also suggests a typical brittle failure. The decrease of tensile strength and modulus of CNFP5 after carbonization is due to the quality loss and carbonization shrinkage of the PAA matrix and a certain degree of structural damage of the CNT network during the carbonizing process at 900°C. Likewise, the aligned CNFP5 after carbonization presents a tensile strength of 653 MPa, with the retention rate of 79%. However, the Young's modulus of the carbonized aligned-CNFP5 increases to 156 GPa, 54% higher than uncarbonized one. The tensile strength's decrease of aligned CNFP5 may also be caused by the quality loss of PAA and structural damage of CNTs during carbonization. As regards the increase of the Young's modulus, it may ascribe to the highly orientated CNTs and CNT bundles in aligned CNFP5, which may induce the formation of a certain amount of graphite microcrystal from the benzo structures of PAA molecules after carbonization[25, 26].

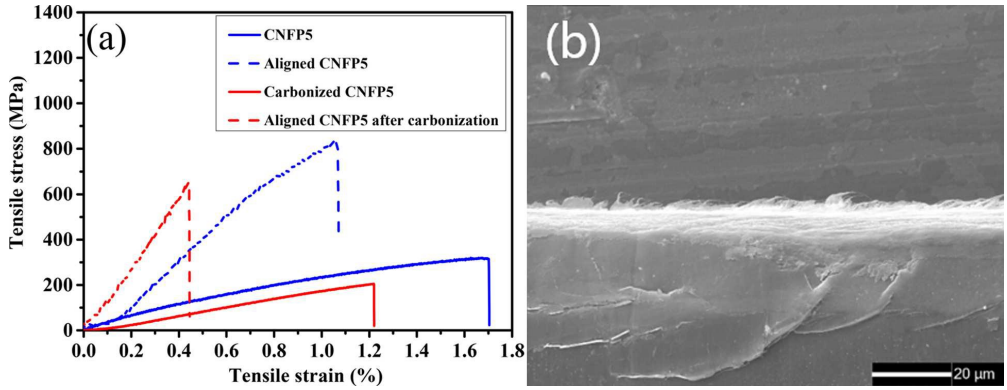

Fig. 9 (a) Tensile stress-strain curves of CNT film/PAA composite before and after carbonization; (b) Fracture morphology of the carbonized nanocomposite.

Thermal and electrical conductivities of CNT film/PAA

Fig. 10a shows through-thickness thermal conductivity of CNT film/PAA composite and pristine CNT film. Though individual CNT has excellent thermal conductivity, the through-thickness thermal conductivity of pristine CNT film is only 0.15 W/(mK) due to its high porosity and weak interaction between CNTs. After the introduction of PAA, the CNFP15 shows a through-thickness thermal conductivity of 1.15 W/(mK), almost seven times higher than pristine CNT film. Moreover, it decreases with reduced PAA content. The thermal conductivity of CNFP5 is only 0.49 W/(mK). After the impregnation of PAA resin, thickness of the nanocomposite film decreased by 50% to 15 µm. The result implies that PAA densifies the stacking of CNTs and fills up the pores. Additionally, conjugated polyene structure of PAA increases the degree of crystallinity and orientation. Thus it enhanced thermal and electric properties of the composite[27]. Thus these effects lead to the increase of the thermal conductivity of the nanocomposite.

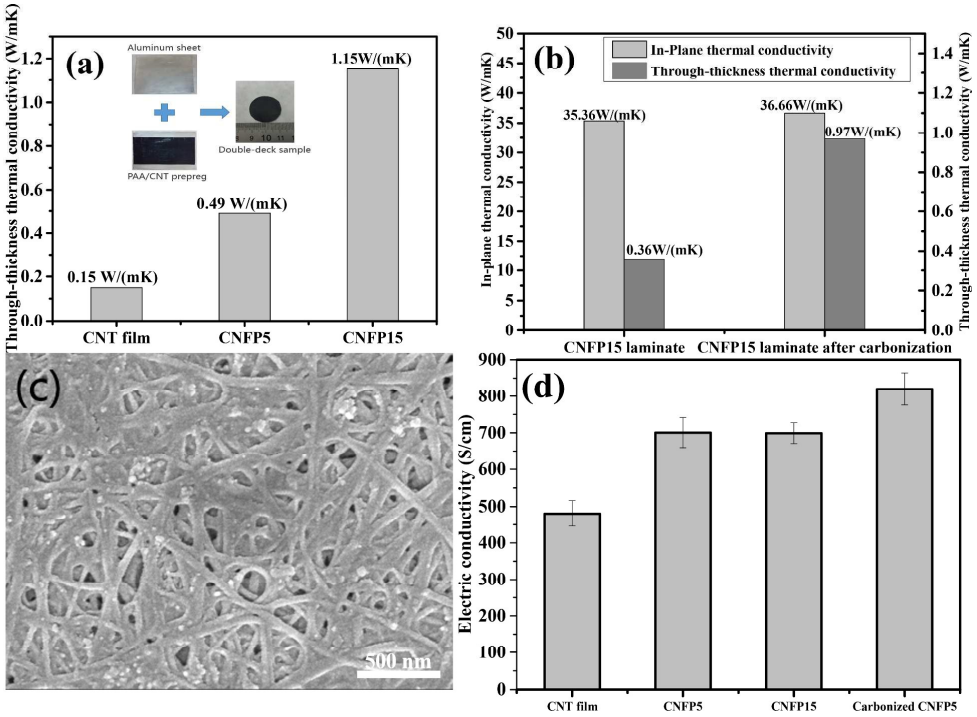

Fig.10 Thermal conductivity of (a) monolayer CNT film/PAA composite and (b) CNFP15 laminate; (c) Surface morphology of CNFP15 after carbonization; (d) Electric conductivity of CNT film and CNT film/PAA composites.

Fig. 10b presents the thermal conductivity of eight-layered CNT film/PAA composite laminate. By comparison with monolayer sample, laminated composite shows lower thermal conductivity due to the introduction of inter-laminar interface. The through-thickness thermal conductivity of laminated CNFP15 decreases to 0.36 W/(mK). Furthermore, an obvious anisotropic feature of thermal conductivity can be also observed. In-plane thermal conductivity of CNFP15 laminate is 35.36 W/(mK). This feature indicates the significant effect of CNT orientation on the thermal conductivity. After carbonization, through-thickness thermal conductivity of the laminate increases significantly to 0.97 W/(mK), almost two times higher than original CNFP15 laminate. The density of carbonized nanocomposite remains 97% of 1.47 g/cm^3 due to the high char yield of PAA, nevertheless it reveals slight porous due to the shrinkage and densification of PAA (Fig. 10c). With the increase of pyrolytic temperature, the ratio of H/C decreases while the carbon content and degree of graphitization of PAA increase[25]. This indicates that the initial insulated polymer structure gradually transforms into conductive graphite crystalline structure during carbonization. As a result, through-thickness interface thermal resistance is reduced effectively. Hence the thermal conductivity is greatly improved after carbonization.

Fig. 10d shows the electric conductivity of CNT film and CNT film/PAA composites. The random lap joints among CNTs can form a conductive path, which enables the CNT film a conductivity of 500 S/cm. After the introduction of PAA, the electric conductivity increases to 700 S/cm for CNFP5 and CNFP15. Additionally, carbonization of PAA made the conductivity of the composite reach up to 820 S/cm.

Conclusions

This paper develops a flexible and heat-resistant nanocomposite in combination of high char yield PAA resin and ductile CNT film. The CNT network in the nanocomposite results in steric hindrance to retard the polymerization of PAA matrix, which effectively reduces the shrinkage and crack defects, and achieves the flexibility of PAA composite. The CNT film/PAA (CNFP5) shows tensile strength and modulus of 303±38 MPa and 22±2 GPa, respectively. Stretching induced alignment of CNTs can further increase the tensile strength and modulus of the nanocomposite up to 830±58 MPa and 101±6 GPa. CNT slippage and network deformation can be hardly induced by tensile stress in CNT film/PAA composite, indicating a lock-up effect of PAA on CNT network to ensure structure stability. Additionally, after a carbonization at 900°C for 0.5h, the nanocomposite remains a retention rate of tensile strength over 66%. Thermogravimetric analysis shows that PAA nanocomposite has a decomposition temperature over 500°C, which is much higher than epoxy or BMI matrix nanocomposite. The char yield after carbonization reaches 90.7%. These features present the excellent heat-resistant performance of CNT film/PAA composite. The through-thickness thermal conductivity reaches 1.15 W/(mK), almost seven times higher than pristine CNT film (i.e. 0.15 W/(mK)). Densification of CNTs stacking and conjugated polyene structure of PAA contribute to the increase of thermal conductivity. Furthermore, after carbonization a certain amount of graphite microcrystal may form from the benzo structures of PAA molecules increasing the thermal conductivity of the nanocomposite, which is two times higher than the uncarbonized one. The electric conductivity of CNT film/PAA composite increases to 700 S/cm, which is 40% higher than pristine CNT film. These performance advantages make CNT film/PAA composite a great potential for multifunctional application in high-heat environment.

Acknowledgements

The authors thank the National Natural Science Foundation of China (Grant No. 51103003, 51273007 and 51403009).

Notes and references

1. M. F. L. De Volder, S. H. Tawfick, R. H. Baughman and A. J. Hart, *Science*, 2013, **339**, 535-539.
2. J. Di, X. Wang, Y. Xing, Y. Zhang, X. Zhang, W. Lu, Q. Li and Y. T. Zhu, *Small*, 2014, **10**, 4606-4625.
3. A. G. Nasibulin, A. Kaskela, K. Mustonen, A. S. Anisimov, V. Ruiz, S. Kivistö, S. Rackauskas, M. Y. Timmermans, M. Pudas, B. Aitchison, M. Kauppinen, D. P. Brown, O. G. Okhotnikov and E. I. Kauppinen, *ACS Nano*, 2011, **5**, 3214-3221.
4. M. Li, Z. Wang, Q. Liu, S. Wang, Y. Gu, Y. Li and Z. Zhang, *Polymer Composites*, 2015.
5. X. Wang, Z. Z. Yong, Q. W. Li, P. D. Bradford, W. Liu, D. S. Tucker, W. Cai, H. Wang, F. G. Yuan and Y. T. Zhu, *Research Letters in Materials Science*, 2013, **1**, 19-25.
6. Z. An, H. Wei, Y. Li and Y. Gao, *Engineering Plastics Application*, 2006, **34**, 19-22.
7. N.-H. Tai, M.-K. Yeh and T.-H. Peng, *Composites Part B: Engineering*, 2008, **39**, 926-932.
8. N.-H. Tai, M.-K. Yeh and J.-H. Liu, *Carbon*, 2004, **42**, 2774-2777.
9. M. H. Choi, I. J. Chung and J. D. Lee, *Chemistry of Materials*, 2000, **12**, 2977-2983.
10. Y. J. Liu, H. P. Teng and Y. L. Guo, *Thermosetting Resin*, 2008.
11. H. Qi, G. Pan, L. Yin, Y. Zhuang, F. Huang and L. Du, *Journal of Applied Polymer Science*, 2009, **114**, 3026-3033.
12. H. Guo, Y. D. Huang and L. Liu, *Chemistry & Adhesion*, 2008.
13. M.-C. Wang and T. Zhao, *Journal of Applied Polymer Science*, 2007, **105**, 2939-2946.
14. S. S. Oishi, E. C. Botelho, C. K. Luscombe and M. C. Rezende, *Polímeros*, 2014, **24**, 541-546.
15. W.-C. Tseng, Y. Chen and G.-W. Chang, *Polymer Degradation and Stability*, 2009, **94**, 2149-2156.

16. M. Liu, L. Gan, F. Zhao, X. Fan, H. Xu, F. Wu, Z. Xu, Z. Hao and L. Chen, *Carbon*, 2007, **45**, 3055-3057.
17. X. Zhang, Y. Huang, T. Wang and L. Liu, *Composites Part A: Applied Science and Manufacturing*, 2007, **38**, 936-944.
18. Q. Liu, M. Li, Y. Gu, Y. Zhang, S. Wang, Q. Li and Z. Zhang, *Nanoscale*, 2014, **6**, 4338-4344.
19. Q. Liu, M. Li, Y. Gu, S. Wang, Y. Zhang, Q. Li, L. Gao and Z. Zhang, *Carbon*, 2015, **86**, 46-53.
20. C. Miao, L. I. Min, S. Wang, J. Yang, G. U. Yizhuo, B. University and Beijing, *Acta Materiae Compositae Sinica*, 2010, **27**, 75-80.
21. A. Moisala, Q. Li, I. A. Kinloch and A. H. Windle, *Composites Science and Technology*, 2006, **66**, 1285-1288.
22. G. R. Anstis, P. Chantikul, B. R. Lawn and D. B. Marshall, *Journal of the American Ceramic Society*, 1981, **64**, 533-538.
23. Q. Wu, J. Bao, C. Zhang, R. Liang and B. Wang, *Journal of Thermal Analysis & Calorimetry*, 2011, **103**, 237-242.
24. X. Ding, *Fiber Composites*, 2005.
25. X. W. Ding, D. Chen, J. H. Cao, Y. Q. Zhuang, J. Wang and Y. S. Jiao, *Polymeric Materials Science & Cngineering*, 2002, **18**, 127-130.
26. R. J. Zaldivar, R. W. Kobayashi, G. S. Rellick and J. M. Yang, *Carbon*, 1991, **29**, 1145–1153.
27. D. Zhang and Y. Zhang, *Journal of Solid Rocket Technology*, 2001.

Graphical Abstract

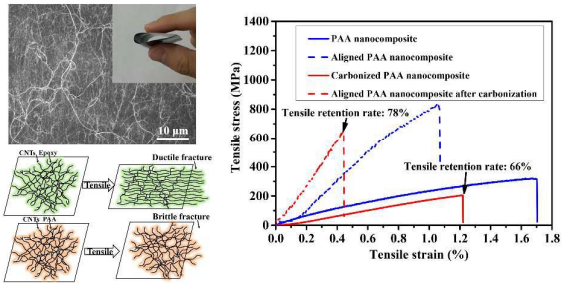

A new nanocomposite with excellent tensile strength, flexibility and heat-resistance.